ELSEVIER

Targeted development of hydrophilic porous polysulfonamide gels with catalytic activity

Sedigheh Alavinia , Ramin Ghorbani-Vaghei [*]

Department of Organic Chemistry, Faculty of Chemistry, Bu-Ali Sina University Hamedan, Iran

ARTICLE INFO

ABSTRACT

We report the use of a template and functional monomers in the synthesis of three novel polysulfonamide gels with new architectures and functional groups. These mesoporous polysulfonamide gels were prepared by the condensation polymerization of benzene-1,3-disulfonyl chloride (as the main precursor), linear monomers, and cross-linkers (as variable precursors) in the presence of a silica template by a combination of sol-gel chemistry and the nanocasting technique. In this synthesis pathway, in situ polymerization onto the template surface led to the construction of a silica/polymer nanocomposite. Next, after removal of the template, the nanocomposite gels were transformed into mesoporous polysulfonamide nanospheres. After the physicochemical identification of the synthesized materials, functionalized polysulfonamides were used as reusable novel catalysts with high efficiency for the Strecker reaction under mild conditions. These polymers have Brønsted/Lewis acid active sites, a mesoporous structure, and hydrogen bonding. Moreover, since these polymers are hydrogels that can absorb water, they can promote the Strecker reaction through chemical absorption of the generated water as a driving force. Overall, this article describes a novel synthesis procedure and application of porous polysulfonamide gels.

1. Introduction

New gel structures fabricated with use of organic material via templates have recently attracted the attention of many researchers. Both template synthesis and self-organization can be used for structuring materials with extension scales. These materials have found tremendous use in basic and applied research, such as sorbents for the adsorption of gas and the removal of organic compounds from water [1]. Owing to the specific features of both polymers and porous gels, the design and synthesis of novel porous polymer gels as a catalyst have attracted much attention. The functional monomers and synthesis processes play an essential role in the engineering of the surface properties and catalytic activity [2–5]. Various methods have been reported for preparing porous polymers; for example, block copolymer self-assembly, template techniques, and a combination of templating and self-assembly techniques [6]. The template techniques have shown high efficiency for the direct replication of the inverse structure of the preformed templates with designed pore architectures as well as pore surface properties and a customized framework [7,8]. These pathways use hard templates that can incorporate several chemical functional groups at the pore surface [6]. Porous cross-linked polymers are excellent candidates for the design

of powerful catalysts because of their ease of handling and processing, high thermal and chemical stabilities, large surface areas, nontoxicity, recyclability, and low-cost production [9].

Several attempts have been made to develop bifunctional organocatalysts that possess sulfonamide hydrogen-bond donors and a basic amine moiety for use in asymmetric reactions [10]. Polysulfonamides are prepared from the reaction between various amines and disulfonyl chloride [11,12]. Cross-linked polysulfonamides are polymers that form a gel structure. Although polysulfonamide as a substrate has found potential applications, there is no report focusing on polysulfonamide gel or cross-linked polysulfonamide in the field of catalysis. Gels are cross-linked polymers that have the ability to absorb different solvents [13]. Cross-linked polysulfonamide is a hydrogel that can promote the Strecker reaction through chemical absorption of the generated water as a driving force [14]. The development of porous multifunctional polysulfonamide gel such as basic amine moiety organocatalysts with effective hydrogen bonding and a large surface area can provide interesting applications for catalytic reactions.

The three-component Strecker reaction is one of the most efficient methods for the synthesis of α-aminonitriles. These materials have been the subject of intense interest in the chemical study of α-amino acids.

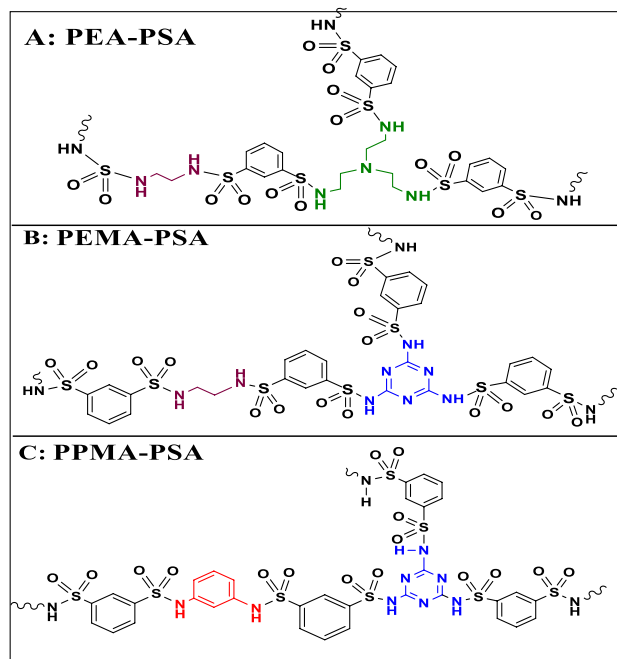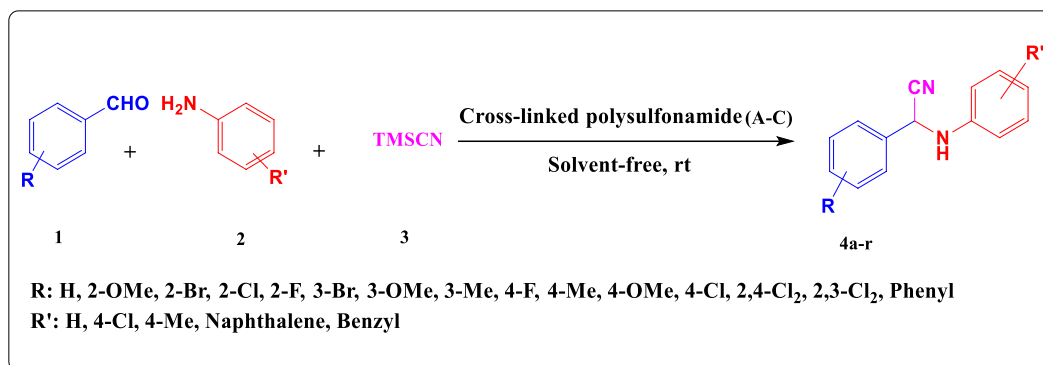**Scheme 1.** Strecker synthesis of α-aminonitrile derivatives and structures of porous cross-linked polysulfonamides. PEA-PSA, poly(ethylene-amine)-polysulfonamide; PEMA-PSA, poly(ethylene-melamine)-polysulfonamide; PPMA-PSA, poly(phenylene-melamine)-polysulfonamide; rt, room temperature; TMSCN, cyanotetramethylsilane.

Several catalysts have been investigated to promote this reaction to achieve efficient and novel protocols for producing α-aminonitriles [15–20]. Therefore, further development of environmental methods for the synthesis of α-aminonitriles is still in great demand. In continuation of our interest in exploring catalytic methods [21], in this study, an efficient and straightforward method for the one-pot synthesis of α-aminonitriles in the presence of three different porous polysulfonamide gels—poly(ethylene-amine)-polysulfonamide (PEA-PSA), poly(ethylene-melamine)-polysulfonamide (PEMA-PSA), and poly (phenylene-melamine)-polysulfonamide (PPMA-PSA)—is described (Scheme 1).

2. Experimental

2.1. Materials

All commercially available chemicals were obtained from Merck and Fluka and were used without further purification otherwise stated. Nuclear magnetic resonance (NMR) spectra were recorded in CDCl$_3$ with a Bruker Avance 400 MHz spectrometer for ^{1}H NMR and a Bruker Avance 100 MHz spectrometer for ^{13}C NMR with tetramethylsilane as an internal standard. Infrared (IR) spectroscopy was conducted with a PerkinElmer GX Fourier transform IR (FT-IR) spectrometer. Mass spectra

were recorded with a Shimadzu QP 1100 BX mass spectrometer. Melting points were determined with a Stuart Scientific SMP3 apparatus. Thermogravimetric analysis (TGA) was performed with a PerkinElmer PYRIS Diamond instrument. The qualitative analysis of the catalysts was performed by energy-dispersive X-ray spectroscopy (EDS) with a Sigma field-emission scanning electron microscope (Zeiss, Germany). Scanning electron microscopy (SEM) was performed with China KYKY-EM3200 instrument operated at 30 kV accelerating voltage. Before the surface area analysis, the samples were activated in a high vacuum at 80 °C for 12 h. All adsorption and desorption measurements were performed at 77 K with a Micromeritics TriStar 3020 version 3.02 (N$_2$) system. The data were analyzed with TriStar II 3020 version 1.03 (Micromeritics, Norcross, GA, USA). The pore size distributions were calculated from the adsorption-desorption isotherms. Wavelength-dispersive X-ray spectroscopy was performed with a TESCAN mira3 instrument. The glass transition temperature (T_g) of the samples was measured by differential scanning calorimetry (DSC; model PL-DSC, Polymer Laboratory Systems, UK). DSC analysis was performed at a heating rate of 10 °C/min in a nitrogen atmosphere with 10.0 mg dried particles.

2.2. Gel content

About 0.5 g of polymer (W_i) was added to the solvent and kept at
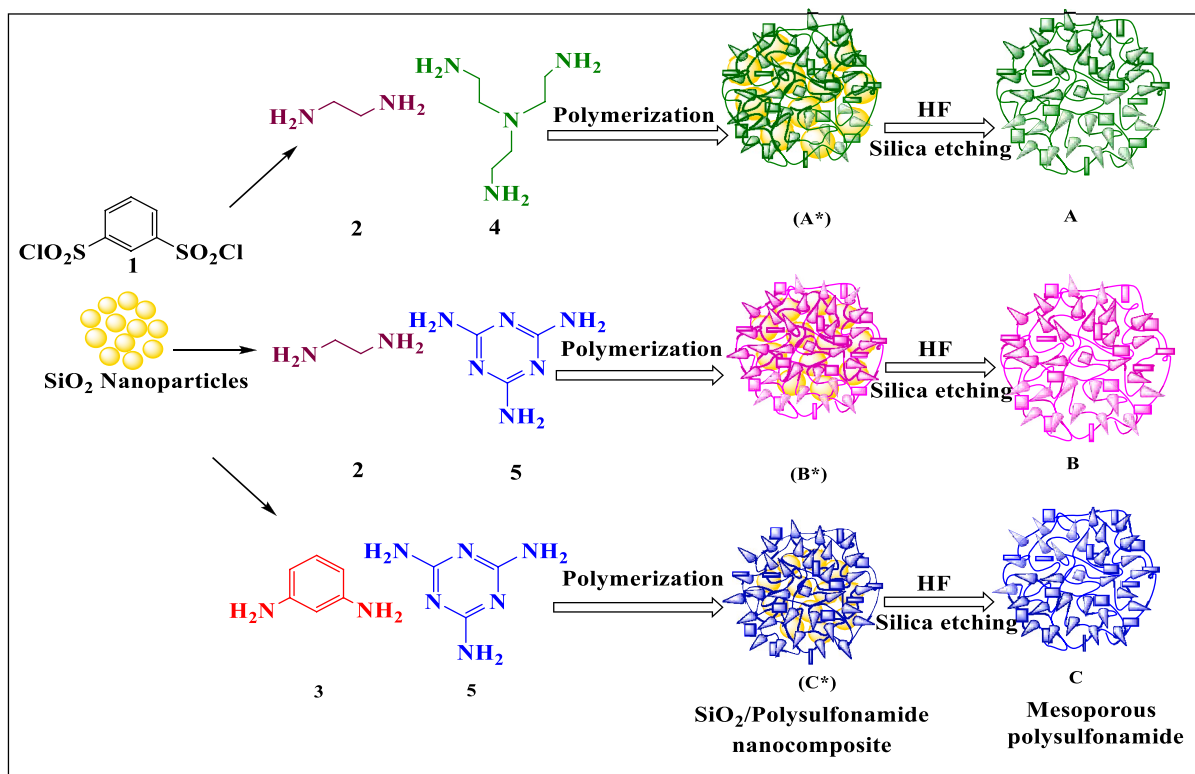
Scheme 2. Preparation of the novel porous polysulfonamide gels with melamine or amine moieties. Formation of self-organized polysulfonamide nanopore: (a) polymerization of polysulfonamide at the surface of silica nanoparticles; (b) extended polymerization leading to surface deposition; (c) selective dissolution of SiO2 by treatment in 5 vol% hydrofluoric acid. A, poly(ethylene-amine)-polysulfonamide; B, poly(ethylene-melamine)-polysulfonamide; C, poly(phenylene-melamine)-polysulfonamide.

room temperature for 24 h. After separation of the swollen part via centrifugation, it was vacuum dried at 40C for 24 h. In the next step, samples were weighed (W_f) and the gel content was calculated according to Eq. (1):

$$\text{Gel content (\%)} = W_i/W_f \times 100. \tag{1}$$

2.3. Synthesis of SiO2 nanoparticles

SiO$_2$ nanoparticles with an average diameter of 20 nm were synthesized in ethanol in accordance with the Stöber method [22]. In summary, 100 mL ethanol, 21.6 mL deionized water, and 2.9 mL aqueous ammonia were added to a round-bottom flask and stirred at ambient temperature for 10 min. Next, about 4.5 mL tetraethyoxysilane was slowly added to the solution by a syringe within 30 min and the reaction was maintained for 10 h. The SiO$_2$ nanoparticles were separated by centrifugation, rinsed with water and ethanol, and then dried under a vacuum at 80 °C for 12 h.

2.4. Synthesis of SiO2/polysulfonamide nanocomposites

SiO$_2$ nanoparticles were modified by in situ polymerization of benzene-1,3-disulfonyl chloride (**1**) (1 mol), 1,3-phenylenediamine (**3**), or ethane-1,2-diamine (NH$_2$CH$_2$CH$_2$NH$_2$) (**2**) (0.7 mol) and 1,3,5-triazine-2,4,6-triamine (**5**) or tris(2-aminoethyl)amine (**4**) (0.3 mol) in the presence of SiO$_2$ nanoparticles (0.1 g). For this purpose, 0.1 g SiO$_2$ nanoparticles and starting material were dispersed homogeneously in 30 mL acetonitrile by ultrasonication. After stirring at room temperature for 6 h, a SiO$_2$/polysulfonamide nanocomposite was obtained (nanocomposites A*, B*, and C* in Scheme 2 were obtained in reflux

conditions). The nanocomposites were filtered off and washed with acetonitrile (20 mL) three times and then dried under a vacuum at room temperature for 12 h.

2.5. Synthesis of porous polysulfonamides

The silica template of the SiO$_2$/polysulfonamide nanocomposite prepared as described in the previous section was removed selectively through etching of the SiO$_2$ nanoparticles with an HF aqueous solution. Then 0.5 g SiO$_2$/polysulfonamide nanoparticle and deionized water (10 mL) were placed in a plastic tube. Next, HF solution (10 mL, 10 wt%) was added to the mixture, and the resulting mixture was magnetically stirred for 6 h. The porous gels created were washed with water, dried at 50 °C, and sieved through an 80-mesh screen.

2.6. Synthesis of α-aminonitriles

PEA-PSA, PEMA-PSA, and PPMA-PSA (50 mg) as catalysts were added to a mixture of substituted benzaldehyde (1 mmol), substituted anilines (1 mmol), and cyanotetramethylsilane (1.2 mmol) under solvent-free conditions at room temperature. Once the reaction had finished, boiling hexane (10 mL) was added to the mixture, and the catalyst was recovered by washing with acetone and then oven dried at 50C to be used six times. The pure product was obtained by crystallization from hexane.

3. Results and discussion

3.1. Characterization of porous polymeric gels as a heterogeneous catalyst

Scheme 2 provides a schematic representation of the preparation of the catalyst. Mesoporous polysulfonamide gels were prepared via the
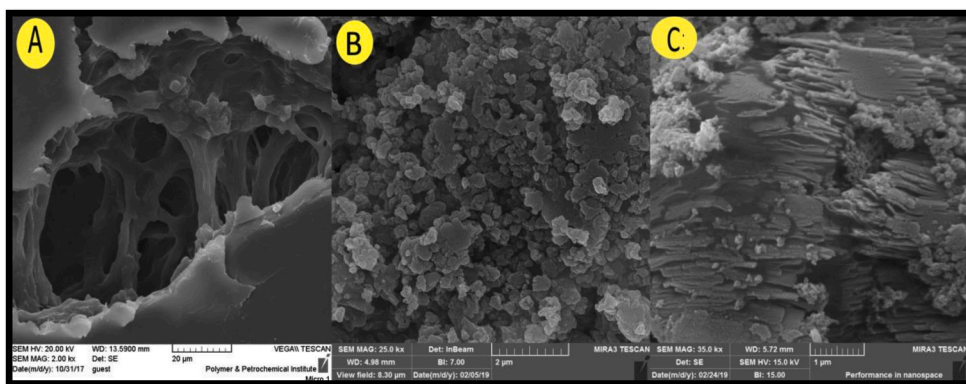
Fig. 1. Field-emission scanning electron microscopy images of (A) porous (A) poly(ethylene-amine)-polysulfonamide gel, (B) porous poly(ethylene-melamine)-polysulfonamide gel, and (C) porous poly(phenylene-melamine)-polysulfonamide gel.
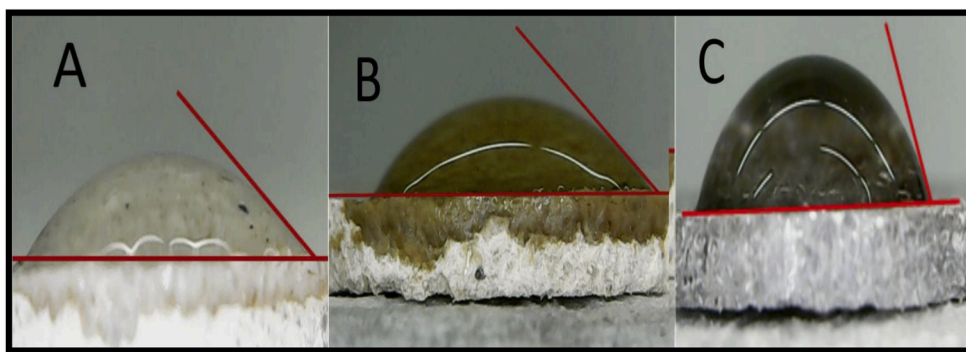

Fig. 2. Contact angles of nanopore water droplets on (A) poly(ethylene-melamine)-polysulfonamide hydrogel, (B) poly(ethylene-amine)-polysulfonamide hydrogel, and (C) poly(phenylene-melamine)-polysulfonamide hydrogel.
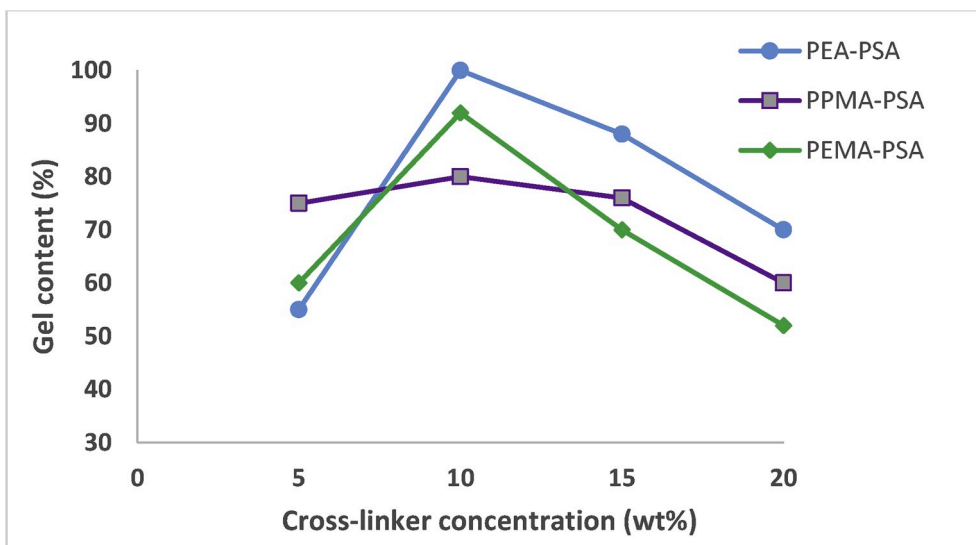

Fig. 3. Swelling behaviors of porous polysulfonamides in water as a function of cross-linker content: poly(ethylene-amine)-polysulfonamide (PEA-PSA) with 10 wt% N', N'-bis(2-aminoethyl)ethane-1,2-diamine and 70 wt% ethylenediamine; poly(ethylene-melamine)-polysulfonamide (PEMA-PSA) with 10 wt% melamine and 70 wt% ethylendiamine; and poly(phenylene-melamine)-polysulfonamide (PPMA-PSA) with 10 wt% melamine and 70 wt% phenylenediamine.

condensation polymerization of benzene-1,3-disulfonyl chloride (as the main precursor) and functionalized monomers (as variable precursors) in the presence of a silica template, followed by template removal with hydrofluoric acid. In the synthesis of polysulfonamide gels, melamine and tris(2-aminoethyl)amine were used as cross-linkers. The cross-link is

a bond that links one polymer chain to another [13]. Therefore, the final structure of the polysulfonamides was controlled by three major factors: (1) the properties of the silica template such as surface chemistry and pore size, (2) the cross-linking density of the polymeric framework, and (3) appropriate selection of the monomers. In this work, we concentrate
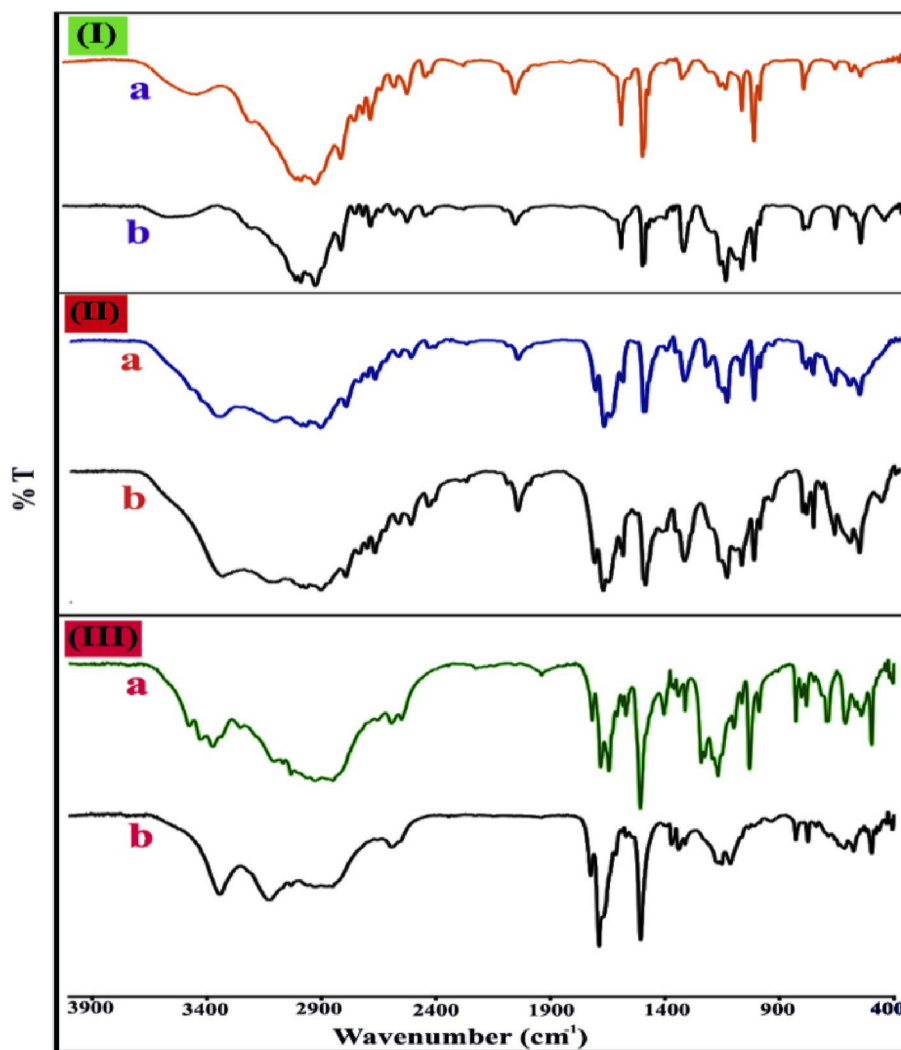
Fig. 4. Fourier transform infrared spectra of (I) SiO$_2$/poly(ethylene-amine)-polysulfonamide (PEA-PSA) (a) and porous PEA-PSA (b), (II) SiO$_2$/poly(ethylene-melamine)-polysulfonamide (PEMA-PSA) (a) and porous PEMA-PSA (b), and (III) SiO$_2$/poly(phenylene-melamine)-polysulfonamide (PPMA-PSA) (a) and porous PPMA-PSA (b).
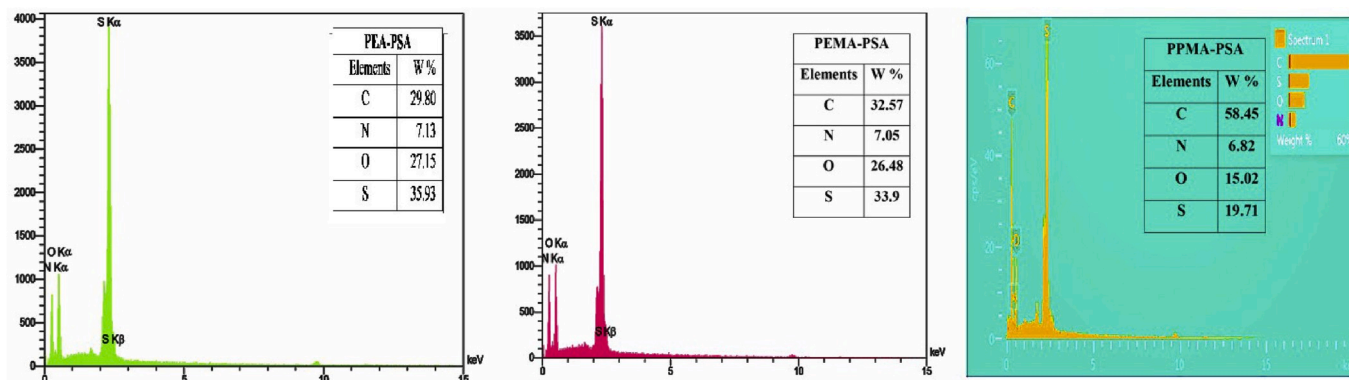

Fig. 5. Energy-dispersive X-ray spectra of the polymeric catalysts. PEA-PSA, poly(ethylene-amine)-polysulfonamide; PEMA-PSA, poly(ethylene-melamine)-polysulfonamide; PPMA-PSA, poly(phenylene-melamine)-polysulfonamide.

mainly on mesoporous multifunctional polysulfonamides as an effective organocatalyst based on an amine/melamine moiety, acidic sulfonamide protons, and sulfonamide hydrogen-bond donors.

3.2. Morphology and wettability of hydrophilic porous polysulfonamide gels

Morphological characterization of the polysulfonamide gels was performed by field-emission SEM (FE-SEM). Fig. 1 shows FE-SEM images
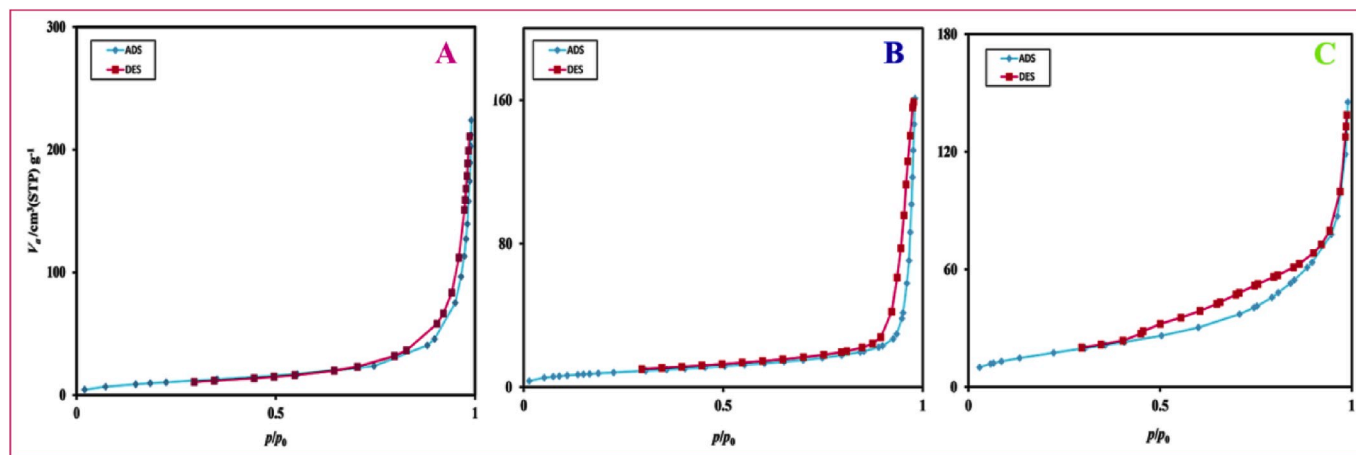
Fig. 6. N_2 adsorption (ADS)-desorption (DES) isotherms for (A) poly(ethylene-amine)-polysulfonamide, (B) poly(ethylene-melamine)-polysulfonamide, and (C) poly (phenylene-melamine)-polysulfonamide.

Table 1
Texture parameters obtained from nitrogen adsorption-desorption studies.

Sample	BET surface area ($m^2\ g^{-1}$)	Pore diameter by BJH method (nm)	Pore volume ($cm^3\ g^{-1}$)
PEA-PSA	560	56.36	0.43
PEMA-PSA	381	48.80	0.37
PPMA-PSA	265	39.78	0.24

BET, Brunauer-Emmett-Teller; BJH, Barrett-Joyner-Halenda; PEA-PSA, poly (ethylene-amine)-polysulfonamide; PEMA-PSA, poly(ethylene-melamine)-polysulfonamide; PPMA-PSA, poly(phenylene-melamine)-polysulfonamide.

of porous cross-linked polysulfonamides. The treated samples exhibited a porous structure with nanoscale pores. As shown in Fig. 1A, porous PEA-PSA has the greatest pore volume. According to Fig. 1A, an increase in pore size and pore volume occurred because of the flexible aliphatic chain of the polysulfonamide matrix in PEA-PSA. On the other hand, because of the aromatic framework in PPMA-PSA, the pore size and pore volume (Fig. 1C) decreased. Therefore, polymer components resulted in significant changes in the morphology and porosity of the

polysulfonamides.

The wettability was examined by our measuring the contact angle. Fig. 2 presents the contact angles of water droplet samples. The contact angle between water and polymers was less than 90°, which indicates good hydrophilicity behavior. The contact angles are 33°, 43°, and 65°, respectively, for PEA-PSA (Fig. 2A), PEMA-PSA (Fig. 2B), and PPMA-PSA (Fig. 2C) [23].

3.3. Gel content

A higher swelling capacity and a higher swelling rate are needed in real-world applications. The solvent-holding capacity of gels is mostly attributed to the presence of hydrophilic groups such as amino, sulfonamide, and melamine groups in the polymer networks. Our studying gel content diagrams of the porous polysulfonamide gels revealed good compatibility with water. According to Fig. 3, the gel content was increased for a cross-linker concentration ranging from 5% to 10% and decreased for cross-linker concentrations higher than 10%. According to these data, with the small amount of cross-linker, the swelling ratio was low, because a gel with low cross-link density is unable to keep the absorbed solvent because of insufficient network volume. On increase of cross-linker concentration, the gel content of the polymers was
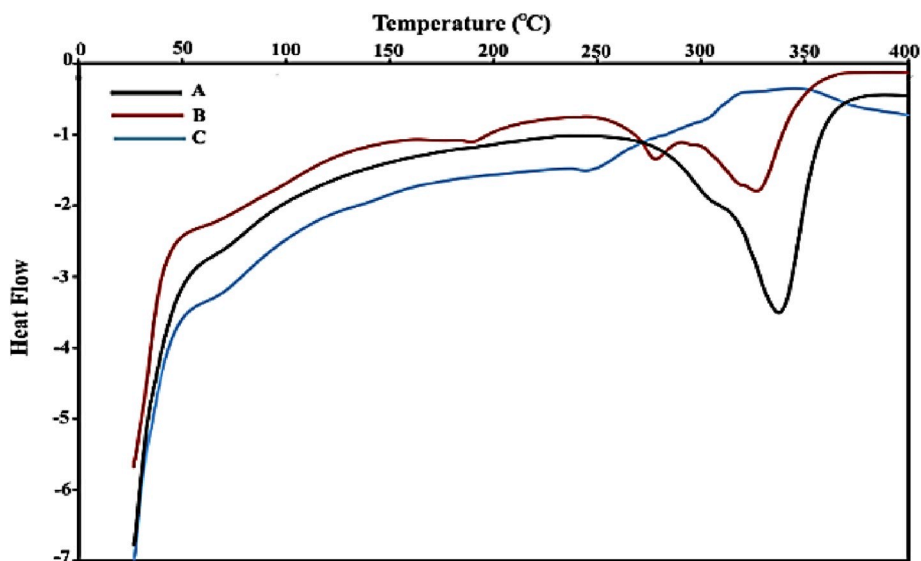

Fig. 7. Three differential scanning calorimetry scans for samples with various monomers and cross-linkers: (A) poly(ethylene-amine)-polysulfonamide; (B) poly (ethylene-melamine)-polysulfonamide; (C) poly(phenylene-melamine)-polysulfonamide.
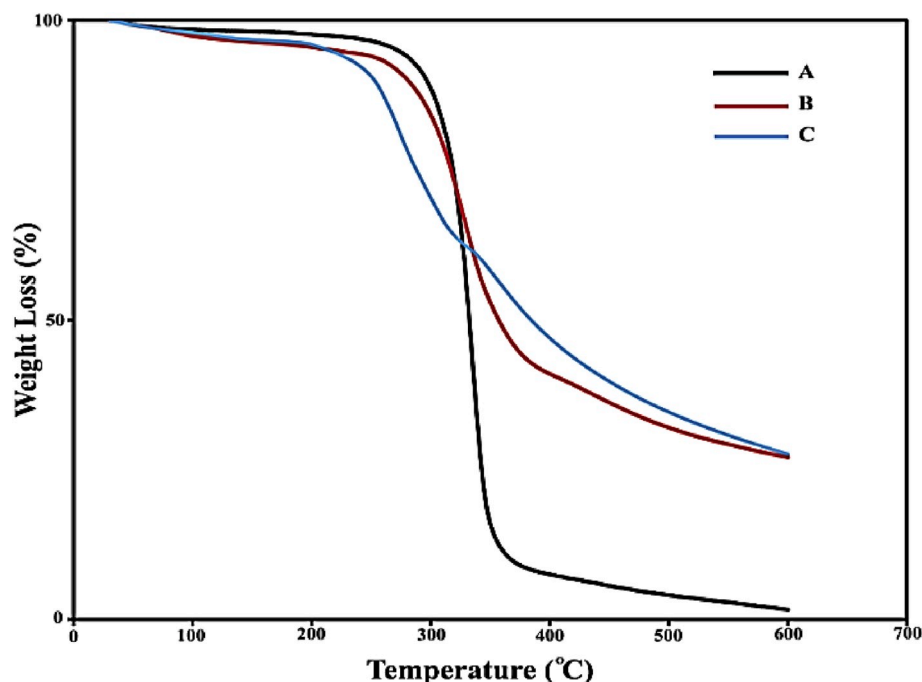
Fig. 8. Thermogravimetric analysis thermograms of porous polysulfonamide gels: (A) poly(ethylene-amine)-polysulfonamide; (B) poly(ethylene-melamine)-polysulfonamide; (C) poly(phenylene-melamine)-polysulfonamide.

Table 2
Optimized results for the synthesis of α-aminonitrile **4a**[a].

Entry	Catalyst (mg)	Conditions	Time (min)	Yield (%)[b] PEA-PSA PEMA-PSA PPMA-PSA
1	–	Solvent-free, rt	120	– – –[c]
2	25	Solvent-free, rt	60	58 65 70
3	50	Solvent-free, rt	15	80 85 92
4	100	Solvent-free, rt	15	80 85 92
5	50	EtOH	30	71 75 80
6	50	CH₃CN	15	77 80 83
7	50	Toluene	60	65 68 75
8	50	H₂O	60	52 61 65
9	50	Solvent-free, 50 °C	15	80 85 92

PEA-PSA, poly(ethylene-amine)-polysulfonamide; PEMA-PSA, poly(ethylene-melamine)-polysulfonamide; PPMA-PSA, poly(phenylene-melamine)-polysulfonamide; rt, room temperature.
[a] Reaction conditions: 1 mmol benzaldehyde, 1 mmol aniline, and 2 mmol cyanotetramethylsilane under solvent-free condition at room temperature.
[b] Isolated yield.
[c] No reaction occurred.

gradually increased such that at 10% cross-linker concentration the greatest absorbency was achieved. When the cross-linker concentration was increased to more than 10%, the pores inside the gel became smaller and, as a result, the gel content decreased. The swelling behavior may be due to the hydrophilicity and large specific surface area of the synthesized polymeric gels [24] (Fig. 3).

3.4. FT-IR spectra

From Fig. 4, which shows the FT-IR spectra of the SiO_2/polysulfonamide and porous polysulfonamide samples, the following can be confirmed: (1) the presence of SiO_2, –S═O, and –NH functional groups; (2) successful polymerization; (3) cross-linking; and (4) and removal of the template to create porous polysulfonamides. The characteristic peak of SiO_2 appears at 1112, 1100, and 1150 cm^{-1}, and is attributed to Si–O stretching vibrations of silica nanoparticles for SiO_2/PEA-PSA, SiO_2/

PEMA-PSA, and SiO_2/PPMA-PSA, respectively [25] (Fig. 4, panels I–III, spectra a). This peak does not appear in the FT-IR spectra of the porous polysulfonamides (Fig. 4, panels I–III, spectra b) because of the complete removal of the template from the nanocomposite. The presence of absorption bands at 1654 and 1684 cm^{-1} for PEMA-PSA and at 1681 and 1684 cm^{-1} for PPMA-PSA shows that these polymers were successfully modified by a cross-linker (melamine) (Fig. 4, panels II and III, spectra b). The spectra of the porous polymers indicate S═O stretching vibrations at 1148 and 1334 cm^{-1} for PEA-PSA, at 1168 and 1312 cm^{-1} for PEMA-PSA, and at 1155 and 1333 cm^{-1} for PPMA-PSA [11,12].

3.5. Energy dispersive X-ray spectra

The EDS analysis of the cross-linked polysulfonamides (Fig. 5) reveals the signals of sulfur, nitrogen, oxygen, and carbon in the structure of the polymeric catalyst. Comparison of the EDS results indicated that the Si atom was removed from the silica particles coated with polysulfonamide by the HF etching.
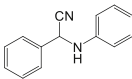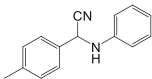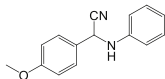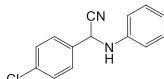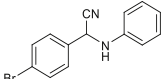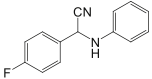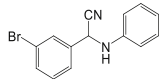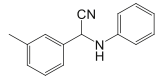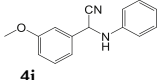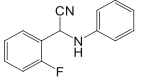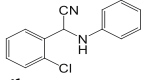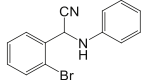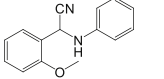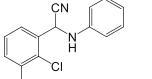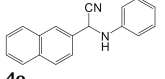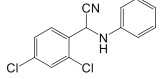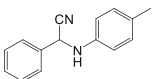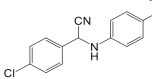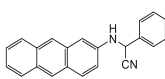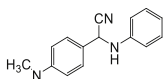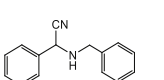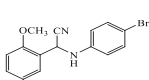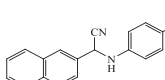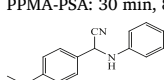
3.6. N_2 adsorption and desorption

To determine the textural properties, the N_2 adsorption-desorption isotherms of the polysulfonamides were measured (Fig. 6). All of the N_2 isotherms are similar and reveal the typical type IV isotherm with type H3 hysteresis (defined by IUPAC), which identified the materials as mesoporous (Fig. 6) [26]. Table 1 summarizes the results of N_2 adsorption-desorption, including pore diameters (Barrett-Joyner-Halenda method), the Brunauer-Emmett-Teller surface area, and the total pore volume of the samples studied. These results are in good agreement with the FE-SEM results.

3.7. Thermogravimetric properties and DSC results

Fig. 7 illustrates three DSC scans for the functionalized polysulfonamides. From Fig. 7, all the polysulfonamide samples have a glass transition temperature. In PEA-PSA (Fig. 7, scan A), with a higher percentage of the network and a higher molecular weight, the glass

Table 3

Synthesis of α-aminonitriles **4a**–**4x** with porous polymeric composite[a].

4a
PEA-PSA: 15 min, 80%[b]
PEMA-PSA: 15 min, 85%
PPMA-PSA: 15 min, 92%

4b
PEA-PSA: 20 min, 78%
PEMA-PSA: 20 min, 85%
PPMA-PSA: 20 min, 90%

4c
PEA-PSA: 20 min, 72%
PEMA-PSA: 20 min, 80%
PPMA-PSA: 20 min, 88%

4d
PEA-PSA: 10 min, 86%
PEMA-PSA: 10 min, 91%
PPMA-PSA: 10 min, 95%

4e
PEA-PSA: 10 min, 82%
PEMA-PSA: 10 min, 88%
PPMA-PSA: 10 min, 95%

4f
PEA-PSA: 20 min, 80%
PEMA-PSA: 20 min, 88%
PPMA-PSA: 20 min, 92%

4g
PEA-PSA: 25 min, 80%
PEMA-PSA: 25 min, 83%
PPMA-PSA: 25 min, 88%

4h
PEA-PSA: 25 min, 75%
PEMA-PSA: 25 min, 80%
PPMA-PSA: 25 min, 85%

4i
PEA-PSA: 25 min, 72%
PEMA-PSA: 25 min, 78%
PPMA-PSA: 25 min, 84%

4j
PEA-PSA: 25 min, 70%
PEMA-PSA: 25 min, 77%
PPMA-PSA: 25 min, 80%

4k
PEA-PSA: 25 min, 74%
PEMA-PSA: 25 min, 83%
PPMA-PSA: 25 min, 85%

4l
PEA-PSA: 25 min, 72%
PEMA-PSA: 25 min, 80%
PPMA-PSA: 25 min, 83%

4m
PEA-PSA: 25 min, 72%
PEMA-PSA: 25 min, 75%
PPMA-PSA: 25 min, 77%

4n
PEA-PSA: 20 min, 85%
PEMA-PSA: 20 min, 90%
PPMA-PSA: 20 min, 94%

4o
PEA-PSA: 30 min, 78%
PEMA-PSA: 30 min, 83%
PPMA-PSA: 30 min, 88%

4p
PEA-PSA: 15 min, 87%
PEMA-PSA: 15 min, 90%
PPMA-PSA: 15 min, 94%

4q
PEA-PSA: 10 min, 85%
PEMA-PSA: 10 min, 87%
PPMA-PSA: 10 min, 90%

4r
PEA-PSA: 35 min, 73%
PEMA-PSA: 35 min, 80%
PPMA-PSA: 35 min, 86%

4s
PEA-PSA: 30 min, 70%
PEMA-PSA: 30 min, 75%
PPMA-PSA: 30 min, 83%

4t
PEA-PSA: 30 min, 72%
PEMA-PSA: 30 min, 80%
PPMA-PSA: 30 min, 84%

4u
PEA-PSA: 10 min, 83%
PEMA-PSA: 10 min, 89%
PPMA-PSA: 10 min, 94%

4v
PEA-PSA: 40 min, 75%
PEMA-PSA: 40 min, 82%
PPMA-PSA: 40 min, 86%

4w
PEA-PSA: 30 min, 70%
PEMA-PSA: 30 min, 75%
PPMA-PSA: 30 min, 82%

4x
PEA-PSA: 30 min, 72%
PEMA-PSA: 30 min, 82%
PPMA-PSA: 30 min, 87%

PEA-PSA, poly(ethylene-amine)-polysulfonamide; PEMA-PSA, poly(ethylene-melamine)-polysulfonamide; PPMA-PSA, poly(phenylene-melamine)-polysulfonamide.
[a] Reaction conditions: 1 mmol aldehyde, 1 mmol aniline, and 1.2 mmol cyanotetramethylsilane under solvent-free conditions at room temperature.
[b] Isolated yield.

transition temperature shows a gradual rise (71C) [27]. Accordingly, the reduction in the cross-link density leads to the glass transition shifting to lower temperatures for PEMA-PSA (Fig. 7, scan B; 64C) and PPMA-PSA (Fig. 7, scan C; 60C).

Fig. 8 presents the TGA of the prepared polymeric samples. As can be seen from Fig. 8, a significant weight loss occurs at 210–400C for PEA-PSA (thermogram A) and at 270–360C for PEMA-PSA (thermogram B) and PPMA-PSA (thermogram C). This weight loss is mainly due to the loss of organic moieties [12]. Fig. 8 shows that the thermal stability of PEMA-PSA and PPMA-PSA is lower than that of PEA-PSA. Hence, it is concluded that the amount of cross-linked polymer in and the molecular mass of PPMA-PSA and PEMA-PSA are probably less than those of PEA-PSA.

3.8. Catalytic activity

The catalytic effect of PEA-PSA, PEMA-PSA, and PPMA-PSA nano-composites was investigated in the synthesis of 2-phenyl-2-(phenyla-mino)acetonitrile **4a** as a model compound (Table 2). First, on the basis of our observations, in the absence of the catalyst, the reaction could not proceed even after a long reaction time (entry 1). So, the catalyst content was studied, and it found that 50 mg catalyst is the optimal amount for this reaction (entry 3). A catalyst content less than 50 mg resulted in a low reaction yield (entry 2). In addition, the yield of the product did not increase when the catalyst content was increased to more than 50 mg (entry 4). The experimental results in Table 1 revealed that room temperature and solvent-free conditions were the optimum reaction variables (entry 3), while use of water, ethanol, toluene, and acetonitrile as the solvent resulted in reduced yields (entries 5–8). Further increase of the temperature to 50 °C did not have a significant effect on the yield (entry 9). This catalytic activity is probably because of the acidity of –NH, which is controlled by melamine groups and the resonance effect on SO_2, as well as the basicity and hydrogen bonding. On the basis of the results and reaction yields, the hydrogen acidic strength and the amount of hydrogen bonds per unit area of the poly-mers are as follows: PPMA-PSA > PEMA-PSA > PEA-PSA. This could be due to the high density of hydrogen bonds and more acidic strength in PPMA-PSA and PEMA-PSA than in PEA-PSA.
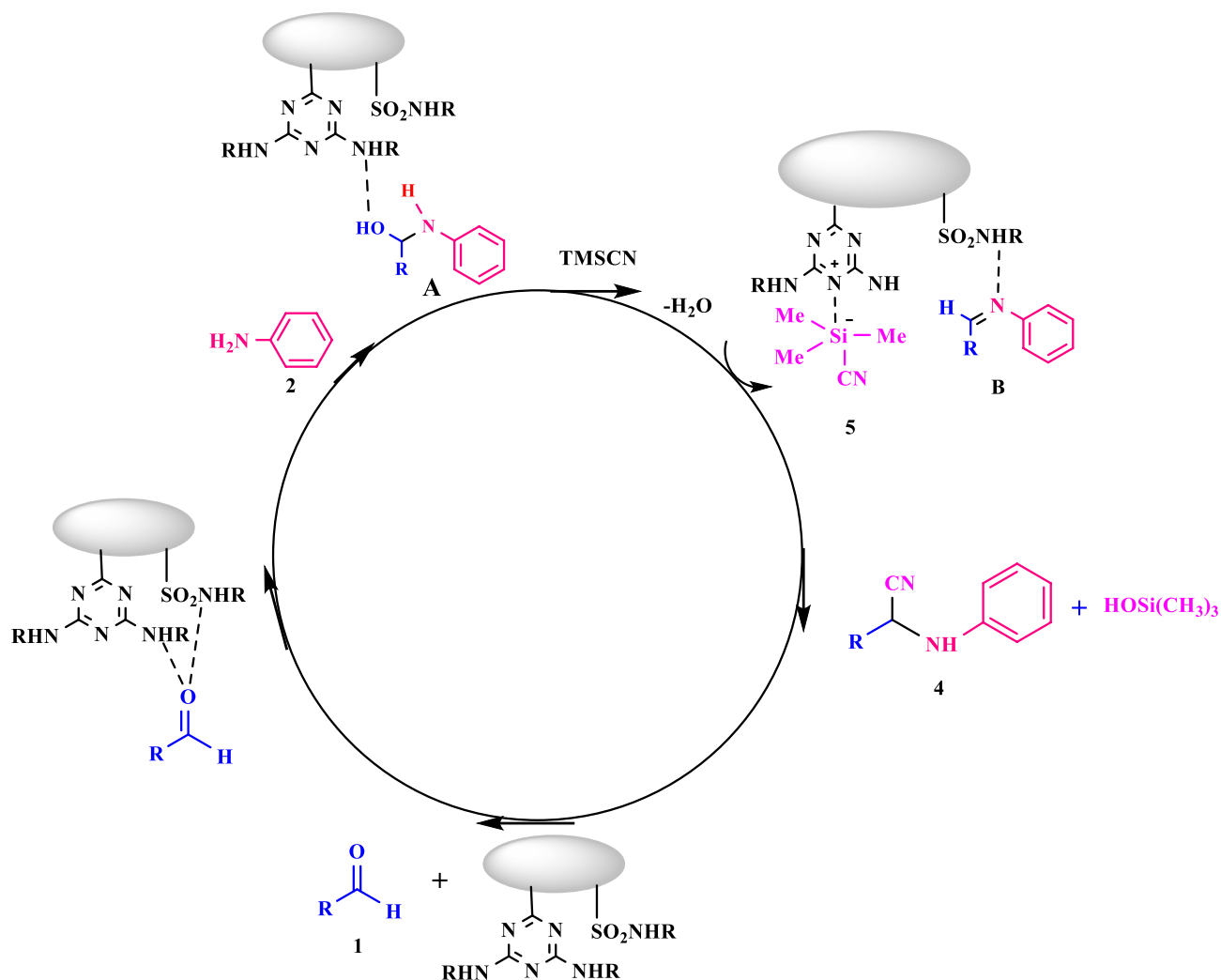
Scheme 3. Suggested mechanism for the synthesis of α-aminonitriles catalyzed by poly(ethylene-melamine)-polysulfonamide. TMSCN, cyanotetramethylsilane.

Table 4
Comparison of different methods for the synthesis of 2-phenyl-2-(phenylamino) acetonitrile **4a**.

Catalyst	Conditions	Time (min)	Yield[a] (%)	Reference
Cross-linked polysulfonamide (PEA-PSA, PEMA-PSA, PPMA-PSA, 50 mg)	Solvent-free, rt	15	80, 85, 92 (92, 92, 91, 91, 90, 90)[b]	This work
Fe_3O_4@ZrO_2/SO_4^{2-} (60 mg)	EtOH, rt	30	95	[19]
Sulfated polyborate (5 mol %)	Solvent-free, rt	2	98	[18]
Polyboric acid	Solvent-free, 90 °C	15	98	[18]
PVP-SO_2 complex (100 mg)	CH_2Cl_2, 50 °C	360	89	[29]
Fe_3O_4@cellulose-OSO_3H (50 mg)	CH_3CN, rt	15	87	[30]
MNPs with urethane moieties	Solvent-free, 50 °C	30	87	[28]

MNP, magnetic nanoparticles; PEA-PSA, poly(ethylene-amine)-polysulfonamide; PEMA-PSA, poly(ethylene-melamine)-polysulfonamide; PPMA-PSA, poly(phenylene-melamine)-polysulfonamide; PVP, poly(4-vinyl pyridine); rt, room temperature; @, Coated.

[a] Isolated yield.
[b] Recyclability of PPMA-PSA.

These results motivated us to examine the generality of this approach for different aromatic aldehydes and anilines under optimized conditions. According to Table 3, a broad substrate scope is observed for both electron-donating and electron-withdrawing substituents. Overall, it was observed that substituted aldehydes containing electron-withdrawing groups reacted faster than aldehydes containing electron-donating groups. Moreover, substituted aromatic amines with electron-donating groups react faster than anilines with electron-

Table 5
Reusability of poly(ethylene-amine)-polysulfonamide (PEA-PSA) poly(ethylene-melamine)-polysulfonamide (PEMA-PSA), and poly(phenylene-melamine)-polysulfonamide (PPMA-PSA) as catalysts in the synthesis of 2-phenyl-2-(phenylamino)acetonitrile.[a]

Run	Yield (%)[b]		
	PEA-PSA	PEMA-PSA	PPMA-PSA
1	80	85	92
2	80	85	92
3	80	83	91
4	79	83	91
5	78	82	90
6	78	82	90

[a] Reaction conditions: 1 mmol benzaldehyde, 1 mmol aniline, and 1.2 mmol cyanotetramethylsilane.
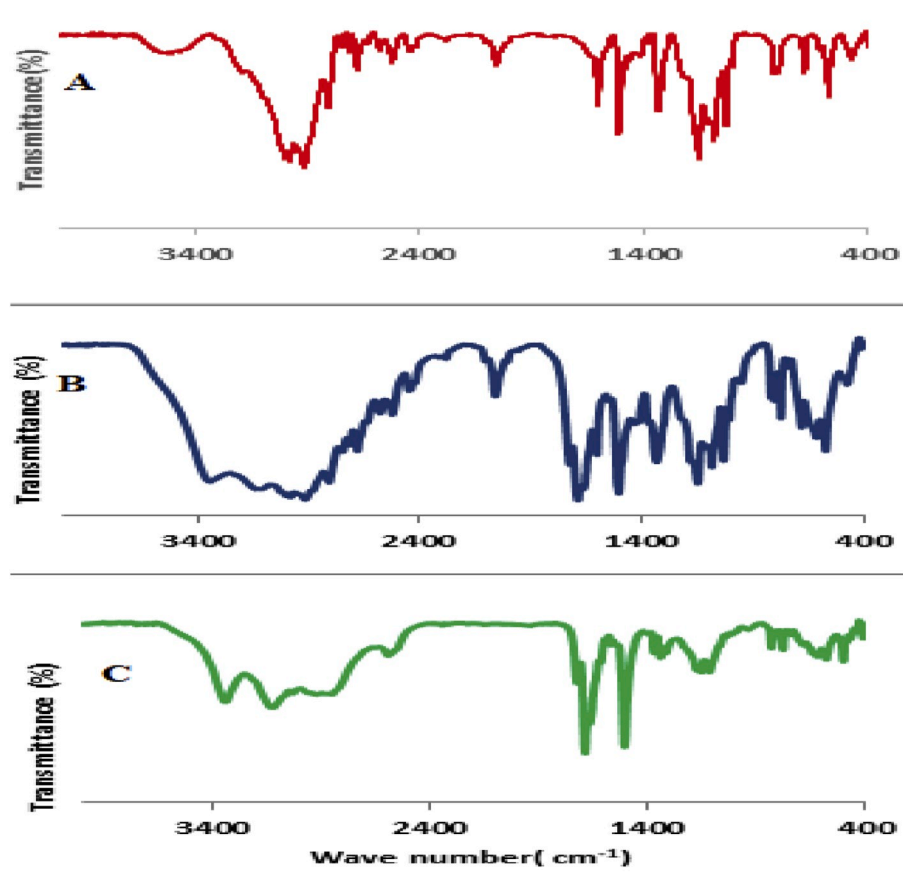[b] Isolated yield.

Fig. 9. Fourier transform infrared spectra of (A) poly(ethylene-amine)-polysulfonamide, (B) poly(ethylene-melamine)-polysulfonamide, and (C) poly(phenylene-melamine)-polysulfonamide after the reaction.

withdrawing groups. All products were examined by means of their spectroscopic data (mass spectrometry, IR spectroscopy, ^{13}C NMR spectroscopy, and ^{1}H NMR spectroscopy).

The proposed reaction mechanism catalyzed by PEMA-PSA is shown in Scheme 3. Several reports confirmed the presence of a dramatic increase in the catalytic activity owing to the good acidic sulfonamide protons and hydrogen bonding [10]. PEMA-PSA appears to be an active catalytic species and is regenerated at the end of the cycle. Initially, the catalyst activates aldehyde **1** through hydrogen bonding, following by the nucleophilic addition of aniline **2** to afford the intermediate **A**, which can promote imine formation through chemical absorption of the generated water [14,28]. In the next step, it was speculated that the catalyst may be effective in activating the imine through hydrogen bonding [14,28]. At this stage, we speculate that the melamine reacts with the silicon atom to form a pentacoordinate derivative [28a]. Moreover, the catalyst facilitates the transfer of the cyanide group to the intermediate **B**. Finally, it was observed that the nucleophilic attack of cyanide anion on the intermediate **B** results in the final product **4** [14, 28]. Once the reaction had finished, boiling hexane (10 mL) was added to the mixture, the catalyst was recovered by washing with *n*-hexane and chloroform, and after separation of the swollen part via centrifugation, it was vacuum dried at 40 °C for 24 h. In the next step, the catalyst was weighed (W_f) and the gel content was calculated. The gel contents are as follows: 80% for PEA-PSA, 70% for PEMA-PSA, and 64% for PPMA-PSA. These results show that catalyst can promote imine formation through chemical absorption of the generated water.

To evaluate the efficiency of the functionalized porous polysulfonamides as catalysts for the Strecker synthesis, the results obtained were compared with those reported in the literature for other catalysts (Table 4). The most noteworthy points of this study include broad

substrate scope, experimental simplicity, reusability of the catalyst, and solvent-free and metal-free conditions at room temperature. The presence of cross-linked polysulfonamides in the catalyst matrix seems absolutely necessary for greater chemical stability of catalysts in comparison with other catalysts in the recycled forms because after several runs, whatever the amount of decomposition, the activity of porous polysulfonamides is greater.

3.9. Catalyst recycling

The reusability and catalytic activity of polymeric catalysts were studied for about six consecutive cycles for the synthesis of 2-phenyl-2-(phenylamino)acetonitrile 4a (Table 5). From FT-IR analysis, the recycled catalyst has high polymer stability during the recycling procedure (Fig. 9).

4. Conclusion

In the present work, three novel classes of hydrophilic polysulfonamides containing a melamine and an amine moiety were synthesized with use of a template and functionalized monomers. Functionalized polysulfonamides with Brønsted/Lewis acid active sites, mesoporous structure, and the possibility of hydrogen bonding were used as a novel reusable catalyst for producing α-aminonitriles with high efficiency under mild reaction conditions. These polymers (i.e., hydrogels with water absorption ability) can accelerate the Strecker reaction through chemical absorption of the produced water. Overall, this article describes a novel synthesis procedure and application of porous polysulfonamide gels.

Declaration of competing interest

The authors declare that they have no known competing financial interests or personal relationships that could have appeared to influence the work reported in this paper.

CRediT authorship contribution statement

Sedigheh Alavinia: Conceptualization, Methodology, Software, Data curation, Writing - original draft, Formal analysis. **Ramin Ghorbani-Vaghei:** Supervision, Conceptualization, Methodology, Validation, Investigation, Formal analysis, Resources, Data curation, Writing - review & editing, Project administration.

Acknowledgments

Appendix A. Supplementary data

Supplementary data to this article can be found online at https://doi.org/10.1016/j.jpcs.2020.109573.

References

[1] (a) D. Wu, F. Xu, B. Sun, R. Fu, H. He, K. Matyjaszewski, Chem. Rev. 112 (2012) 3959–4015;
(b) P.K. Papaioannou, C.S. Karagianni, G. Kakali, V. Charalampopoulos, J. Phys. Chem. Solid. 114 (2018) 246–254.
[2] J. Iocozzia, Z. Lin, Macromolecules 50 (2017) 4906–4912.
[3] L.M. Guo, Y. Wang, Macromolecules 51 (2018) 6248–6256.
[4] S. Mukherjee, M. Das, A. Manna, R. Krishna, S. Das, Chem. Mater. 31 (2019) 3929–3940.
[5] J. Xie, L. Chen, W.H. Wang, P. Wang, C.T. Au, S.F Yin Catal, Sci. Technol. 7 (2017) 1211–1216.
[6] Q. Ye, S. Liu, J. Zhang, F. Xu, F. Zhou, W. Liu, ACS Sustain. Chem. Eng. 14 (2019) 12527–12535.
[7] K. Kim, G. Yoon, S. Baek, J. Rho, H. Lee, ACS Appl. Mater. Interfaces 11 (2019) 26109–26115.
[8] S. Tanaka, Y.V. Kaneti, R. Bhattacharjee, M.N. Islam, R. Nakahata, N. Abdullah, S. Yusa, N.T. Nguyen, M.J.A. Shiddiky, Y. Yamauchi, M.S.A. Hossain, ACS Appl. Mater. Interfaces 10 (2018) 1039–1049.
[9] (a) B. Li, R. Gong, Y. Luo, B. Tan, Soft Matter 7 (2011) 10910–10916;
(b) Y. Lei, M. Zhang, Q. Li, Y. Xia, G. Leng, Polymers 11 (2019), 2091–2033;
(c) Y. Wan, Y. Lei, G. Lan, D. Liu, G. Li, R. Bai, Appl. Catal., A 562 (2018) 267–301;
(d) Y. Lei, Y. Wan, G. Li, X.-Y. Zhou, Y. Gu, J. Feng, R. Wang, Mater. Chem. Front. 1 (2017) 1541–1549.
[10] M. Dajek, R. Kowalczyk, P.J. Boratyński, Catal. Sci. Technol. 8 (2018) 4358–4363.
[11] R. Ghorbani-Vaghei, H. Jalili, Synthesis 7 (2005) 1099–1102.
[12] S. Alavinia, R. Ghorbani-Vaghei, J. Rakhtshah, J.Y. Seyf, I.A. Arabian, Appl. Organomet. Chem. 34 (2020) e5449.
[13] S.S. Sagiri, A.B. Behera, R.R. Rafanan, C. Bhattacharya, K. Pal, I. Banerjee, D. Rousseau, Soft Mater. 12 (2013) 47–72.
[14] M.G. Dekamin, M. Azimoshan, L. Ramezani, Green Chem. 15 (2013) 811–820.
[15] V.V. Kouznetsov, C.E.P. Galvis, Tetrahedron 74 (2018) 773–810.
[16] W. Wang, S. Zhang, S. Hu, D. Wang, W. Gao, R. Cong, T. Yang, Appl. Catal., A 542 (2017) 240–251.
[17] A.M. Nauth, T. Konrad, Z. Papadopulu, N. Vierengel, B. Lipp, T. Opatz, Green Chem. 20 (2018) 4217–4223.
[18] K.S. Indalkar, C.K. Khatri, G.U. Chaturbhuj, Tetrahedron Lett. 58 (2017) 2144–2148.
[19] H. Ghafuri, A. Rashidizadeh, B. Ghorbani, M. Talebi, New J. Chem. 6 (2015) 27–35.
[20] W. Wang, Y. Wang, B. Wu, et al., Catal. Commun. 58 (2015) 174–178.
[21] (a) R. Ghorbani-Vaghei, S. Alavinia, N. Sarmast, Appl. Organomet. Chem. 32 (2018) e4038;
(b) R. Ghorbani-Vaghei, S. Alavinia, Z. Merati, V. Izadkhah, Appl. Organomet. Chem. 32 (2018) e4127.
[22] W. Stöberand, A. Fink, J. Colloid Interface Sci. 26 (1968) 62–69.
[23] Y. Lei, G. Lan, D. Zhu, R. Wang, Zhou X-Y, G. Li, Appl. Organomet. Chem. 32 (2018), e4421.
[24] A. Pourjavadi, M. Doulabi, J. Polym. Sci. Part A Polym. Chem. 52 (2014) 3166–3172.
[25] (a) J. Lin, H. Huang, M. Wang, M.J. Deng, Polym. Chem. 7 (2016) 1675–1681;
(b) X. Yong, Y. Wu, J. Deng, Polym. Chem. 10 (2019) 4441–4448.
[26] K.S.W. Sing, R.T. Williams, Adsorpt. Sci. Technol. 22 (2004) 773–782.
[27] H. Soleimani, R. Bagheri, A. Asadinezhad, Prog. Org. Coating 129 (2019) 278–284.
[28] (a) S. Baghery, M.A. Zolfigol, R. Schirhagl, M. Hasani, M.C.A. Stuart, A. Nagl, Appl. Organomet. Chem. 31 (2017) e3883;
(b) S. Baghery, M.A. Zolfigol, M. Safaiee, D.A. Alonso, A. Khoshnood, Appl. Organomet. Chem. 31 (2017) e3775.
[29] G.A. Olah, T. Mathew, C. Panja, K. Smith, G.K.S. Prakash, Catal. Lett. 114 (2007) 1–7.
[30] A. Maleki, E. Akhlaghi, R. Paydar, Appl. Organomet. Chem. 30 (2016) 382–386.